On the Link Between Central Black Holes, Bar Dynamics, and Dark Matter Halos in Spiral Galaxies

P. Treuthardt[1,2], M. Seigar[1,2], A. Sierra[1], I. Al-Baidhany[1], H. Salo[3], D. Kennefick[2,4], J. Kennefick[2,4], & C. Lacy[2,4]

[1]University of Arkansas at Little Rock, [2]Arkansas Center for Space and Planetary Sciences, [3]University of Oulu, [4]University of Arkansas

University of Arkansas at Little Rock

ABSTRACT

The recent discovery of a relationship between supermassive black hole (SMBH) mass and spiral arm pitch angle (P) shows that SMBHs are tied to the overall secular evolution of a galaxy. Furthermore, the discovery of SMBHs in late-type galaxies with little or no bulge suggests an underlying correlation between the dark matter halo concentration and SMBH mass (M_{BH}), rather than the bulge mass and M_{BH}. The goal of our study is to estimate the theoretical lower limit of the total mass (M_{tot}) of individual galaxies with low central density dark matter haloes, or fast rotating bars. This was done by first measuring P for a sample of 40 barred spiral galaxies from the Carnegie-Irvine Galaxy Survey (CGS; Ho et al. 2011) to determine M_{BH}. M_{tot} is then estimated by the empirical M_{BH}-M_{tot} relation of Bandara et al. (2009). We also produced dynamical simulation models, using K_s-band images to estimate the gravitational potentials, to discern those galaxies with clearly fast rotating bars. We find 7 clear examples and the lower limits to their total mass range from $3 < M_{tot} < 25 \times 10^{11}$ solar masses. We also find that galaxies with low central dark halo densities appear to follow more predictable trends in P, or M_{BH}, versus de Vaucouleurs morphological type index (T) and bar strength versus T than barred galaxies in general. Future work will involve obtaining detailed rotation curves of the 7 galaxies with fast bars and determining if their M_{tot} do indeed exceed the predicted theoretical values.

INTRODUCTION

The connection between the overall morphology and dynamics of galaxies and the centrally located supermassive black holes (SMBHs) they harbor provides a fundamental constraint in the study of galaxy formation and evolution. The recent discovery of a relationship between M_{BH} and spiral arm pitch angle (P; Seigar et al. 2008) shows that SMBHs are tied to the overall secular evolution of a galaxy. The cause of the M_{BH} - P connection is hinted at by the discovery of SMBHs in the centers of late-type galaxies with little or no bulge (Satyapal et al. 2007, 2008). This discovery suggests that the size, or mass, of SMBHs may be tied to the dark matter halo virial mass, or concentration (van den Bosch et al. 2007; Ferrarese 2002). More recently though, Booth & Schaye (2010) have shown that SMBH mass appears to be linked to halo binding energy rather than halo mass.

The secular evolution of a barred spiral galaxy is chiefly influenced by the rotation rate of the non-axisymmetric component (e.g., Kormendy & Kennicutt 2004). Simulation models have shown that after a bar initially forms, the pattern speed (Ω_p) remains fast when embedded in a dark matter halo with a low central density (Debattista & Sellwood 2000). This is due to reduced dynamical friction between the two components that would otherwise cause a rapid decrease in Ω_p. Ω_p also determines the locations of important resonance regions in galaxies with a single perturbation mode, such as a bar. This allows the rotation of a bar to be described by the ratio $\mathcal{R} = R_{CR}/R_{bar}$, where R_{CR} is the corotation resonance radius and R_{bar} is the bar semimajor axis length. When $1 \leq \mathcal{R} \leq 1.4$ a bar is deemed to be a fast rotator, while $\mathcal{R} > 1.4$ implies a slow rotating bar.

METHODS

In order to determine the lower limit of M_{tot} for galaxies with fast bars, we must measure P and determine $\mathcal{R}$ for each galaxy. When P is known, M_{tot} is determined via the Seigar et al. (2008) M_{BH}-P relation as well as the Bandara et al. (2009) M_{BH}-M_{tot} relation.

P was measured using two-dimensional fast Fourier decompositions of the deprojected B-band images and assuming logarithmic spirals (Schröder et al. 1994). The Fourier fits were applied to visually selected annulus regions that range from just beyond the ends of the bars to the outer limits of the visible arms. P is then determined from peaks in the Fourier spectra as this is the most powerful method for finding periodicity in a distribution (Garcia-Gomez & Athanassoula 1993).

Determining $\mathcal{R}$ for each sample galaxy was done by matching the simulated morphology of individual galaxies to B-band images. The models were produced by simulating the behavior of a two-dimensional disk of inelastically colliding gas particles in potentials derived from K_s-band galaxy images. The details of the simulation code we used can be found in Salo et al. (1999) and Salo (1991). We assumed that each galaxy has only one pattern speed, that of the bar, and it was the main parameter that was varied.

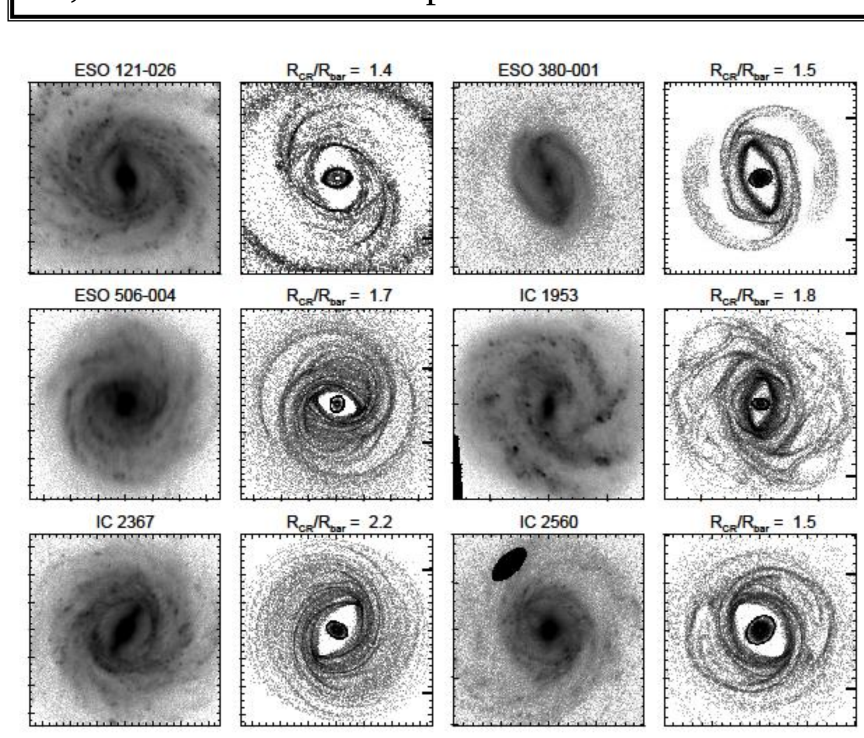

Figure 1: Example of deprojected B-band and best gas particle model images from our sample of galaxies. The models shown correspond to our estimated values of $\mathcal{R}$. Some B-band images display black masks that were used when a foreground star could not be otherwise removed. The thick tick-marks along the right edge of the gas particle images indicate the diameter of corotation.

RESULTS

Table 1. Estimated Galaxy Parameters.

Explanation of columns: (1) Galaxy designation; (2) inclination in degrees derived from fitting ellipses to *B*-band isophotes; (3) bar semimajor axis length in the sky plane, measured in arcseconds, and estimated from ellipse fitting; (4) estimated value and 1σ error of R_{CR}/R_{bar}; (5) spiral arm pitch angle measured by the authors of this paper, ^{a}Seigar et al. 2006, or by ^{b}Block et al. 1999; (6) SMBH mass and mean error in 10^5 solar masses derived from P using equation 2 of Seigar et al. 2008; (7) total mass of the galaxy and mean error in 10^{11} solar masses derived from M_{BH} using equation 8 of Bandara et al. 2009 (*indicates an underestimation of halo mass due to $\mathcal{R} \leq 1.4$ according to Booth & Schaye 2010); (8) de Vaucouleur morphological type index from HyperLeda (Paturel et al. 2003); (9) the maximum of Q_T in the bar region estimated from mass models derived from K_s-band images.

Galaxy (1)	i (2)	R_{bar} (3)	$\mathcal{R}$ (4)	P (5)	M_{BH} (6)	M_{tot} (7)	T (8)	Q_g (9)
ESO 121-026	49.8	20.2	1.38 ± 0.05	10.5 ± 1.2^a	343 ± 119	38.3 ± 8.0	3.9 ± 0.4	0.258
ESO 380-001	60.7	65.5	1.48 ± 0.06	32.3 ± 2.0	12.6 ± 2.8	4.55 ± 1.39	2.8 ± 0.7	0.318
ESO 506-004	62.9	15.0	1.74 ± 0.08	14.0 ± 1.0	148 ± 31	22.3 ± 0.3	2.5 ± 1.0	0.131
IC 1953	48.2	29.3	1.83 ± 0.06	33.0 ± 1.6	11.7 ± 2.2	4.33 ± 1.46	6.1 ± 0.9	0.380
IC 2367	40.9	15.5	2.24 ± 0.06	15.8 ± 0.7	104 ± 14	17.8 ± 1.8	3.1 ± 0.7	0.265
IC 2560	61.7	39.9	1.47 ± 0.06	28.4 ± 4.2	18.7 ± 8.9	5.88 ± 0.54	3.4 ± 0.6	0.112
IC 5240	48.3	39.6	1.50 ± 0.06	24.4 ± 0.9	29.2 ± 3.2	7.83 ± 2.15	1.0 ± 0.3	0.193
IC 5273	48.3	23.3	1.59 ± 0.07	33.5 ± 2.8	11.0 ± 4.1	4.17 ± 0.91	5.7 ± 0.9	0.258
NGC 0151	63.7	18.1	1.40 ± 0.06	36.1 ± 1.5^a	6.98 ± 2.71	3.11 ± 0.81	4.0 ± 0.5	0.105
NGC 0337	41.2	14.8	1.27 ± 0.07	32.9 ± 1.4	11.8 ± 1.9	4.36 ± 1.54*	6.7 ± 0.8	0.800
NGC 0782	30.6	22.8	1.36 ± 0.06	23.7 ± 1.9	31.8 ± 7.6	8.27 ± 1.49	3.0 ± 0.3	0.126
NGC 0945	41.0	17.6	1.66 ± 0.06	15.5 ± 1.3	110 ± 28	18.4 ± 0.4	5.0 ± 0.5	0.301
NGC 1022	20.5	18.4	1.87 ± 0.06	13.7 ± 3.9	158 ± 172	23.2 ± 17.9	1.1 ± 0.3	0.122
NGC 1317	28.3	6.5	1.84 ± 0.06	10.0 ± 0.6	395 ± 70	42.0 ± 4.6	0.8 ± 0.5	0.040
NGC 1723	39.4	18.9	1.87 ± 0.06	21.3 ± 3.4	43.4 ± 22.0	10.1 ± 0.8	1.2 ± 0.6	0.115
NGC 1832	41.0	12.7	1.61 ± 0.08	25.3 ± 6.1	26.3 ± 22.5	7.31 ± 2.10	4.0 ± 0.1	0.226
NGC 2223	24.2	18.6	1.58 ± 0.06	22.8 ± 3.5	35.6 ± 17.2	8.90 ± 0.73	3.8 ± 0.9	0.095
NGC 2525	44.0	14.2	1.78 ± 0.06	22.9 ± 1.9	35.1 ± 8.7	8.82 ± 1.43	5.2 ± 0.5	0.231
NGC 2763	36.5	4.1	1.67 ± 0.08	20.5 ± 2.5	48.6 ± 18.1	10.9 ± 0.6	5.7 ± 0.7	0.235
NGC 3124	35.5	15.0	1.33 ± 0.05	20.5 ± 1.9	48.6 ± 13.5	10.9 ± 1.1*	3.9 ± 0.5	0.209
NGC 3275	28.2	18.6	1.43 ± 0.06	30.0^b	15.9	5.29 ± 2.21	1.9 ± 0.5	0.108
NGC 3347	33.7	13.0	1.73 ± 0.05	37.8 ± 4.1	3.63 ± 5.35	2.04 ± 1.06	3.5 ± 0.8	0.116
NGC 3450	20.2	25.1	1.65 ± 0.06	11.8 ± 0.4^a	244 ± 24	30.8 ± 0.3	3.1 ± 0.4	0.152
NGC 3513	40.5	24.1	1.24 ± 0.07	26.7 ± 3.6^a	22.4 ± 9.4	6.61 ± 0.66*	5.1 ± 0.4	0.540
NGC 3660	42.4	16.3	1.75 ± 0.10	20.4 ± 2.3	49.3 ± 16.9	11.0 ± 0.6	3.9 ± 0.5	0.145
NGC 3887	49.1	16.8	1.89 ± 0.08	24.7 ± 3.7^a	28.2 ± 13.3	7.65 ± 0.64	3.9 ± 0.5	0.143
NGC 4050	50.0	30.0	1.65 ± 0.06	8.9 ± 1.2^a	555 ± 232	52.4 ± 17.2	2.1 ± 0.6	0.203
NGC 4593	45.3	57.0	1.23 ± 0.06	22.9 ± 3.8	35.1 ± 18.6	8.82 ± 0.82*	3.0 ± 0.4	0.181
NGC 5135	28.4	33.2	1.27 ± 0.06	15.8 ± 1.5	104 ± 30	17.8 ± 0.5*	2.4 ± 0.6	0.099
NGC 5156	17.1	9.3	1.61 ± 0.11	20.9 ± 1.6	45.9 ± 10.5	10.5 ± 1.5	3.5 ± 0.9	0.239
NGC 5339	40.0	26.9	1.75 ± 0.08	16.2 ± 2.0	96.6 ± 36.6	16.9 ± 0.9	1.0 ± 0.5	0.255
NGC 5728	53.3	43.8	1.56 ± 0.06	10.3 ± 2.3	362 ± 278	39.8 ± 21.4	1.2 ± 0.7	0.232
NGC 5938	28.3	23.1	1.64 ± 0.06	36.1 ± 9.3	7.0 ± 11.1	3.11 ± 1.73	4.3 ± 0.6	0.151
NGC 6782	23.1	26.7	1.20 ± 0.06	13.4 ± 1.2	168 ± 45	24.2 ± 1.3*	1.0 ± 0.9	0.060
NGC 6923	50.8	11.7	1.31 ± 0.06	23.4 ± 3.7	33.0 ± 16.5	8.47 ± 0.74*	3.1 ± 0.6	0.076
NGC 7059	71.1	41.7	1.72 ± 0.08	17.5 ± 1.3	77.1 ± 17.0	14.6 ± 1.2	5.7 ± 1.0	0.210
NGC 7070	35.4	10.4	1.67 ± 0.16	30.2 ± 5.0	15.6 ± 9.0	5.22 ± 0.67	6.0 ± 0.3	0.183
NGC 7218	66.5	8.8	1.52 ± 0.06	34.3 ± 10.4	9.9 ± 15.5	3.89 ± 2.27	5.6 ± 1.2	0.254
NGC 7392	55.7	19.2	1.44 ± 0.06	24.6 ± 2.0^a	28.5 ± 6.9	7.71 ± 1.47	3.8 ± 0.7	0.177
NGC 7723	48.5	18.9	1.44 ± 0.06	15.7 ± 2.3^a	106 ± 49	18.0 ± 2.2	3.1 ± 0.5	0.243

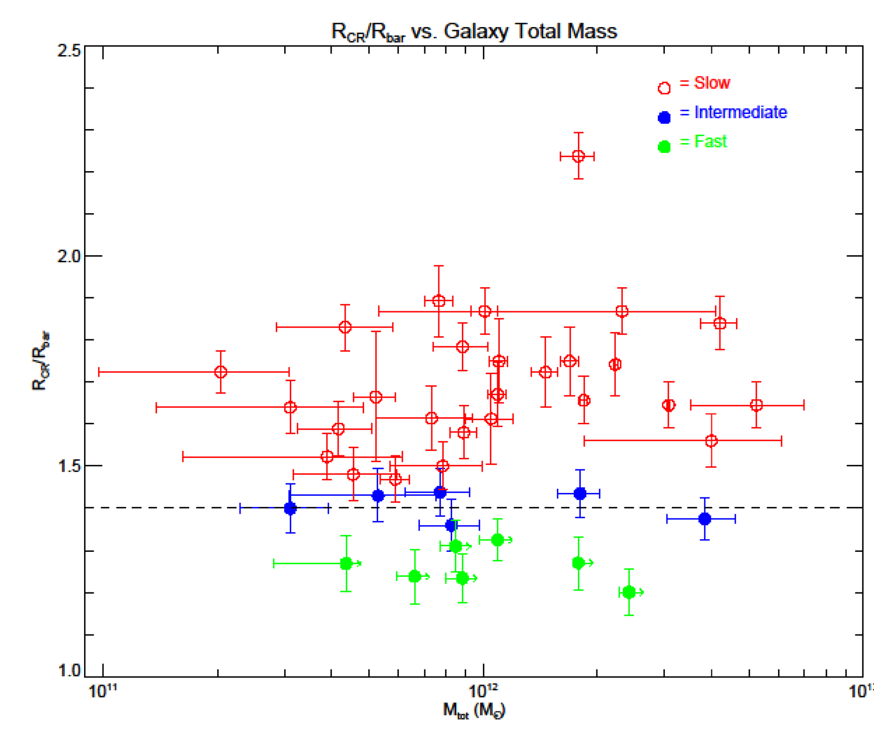

Figure 2: A plot of $\mathcal{R}$ vs. M_{tot} showing the galaxies with fast bars and, thereby, underestimated M_{tot} values.

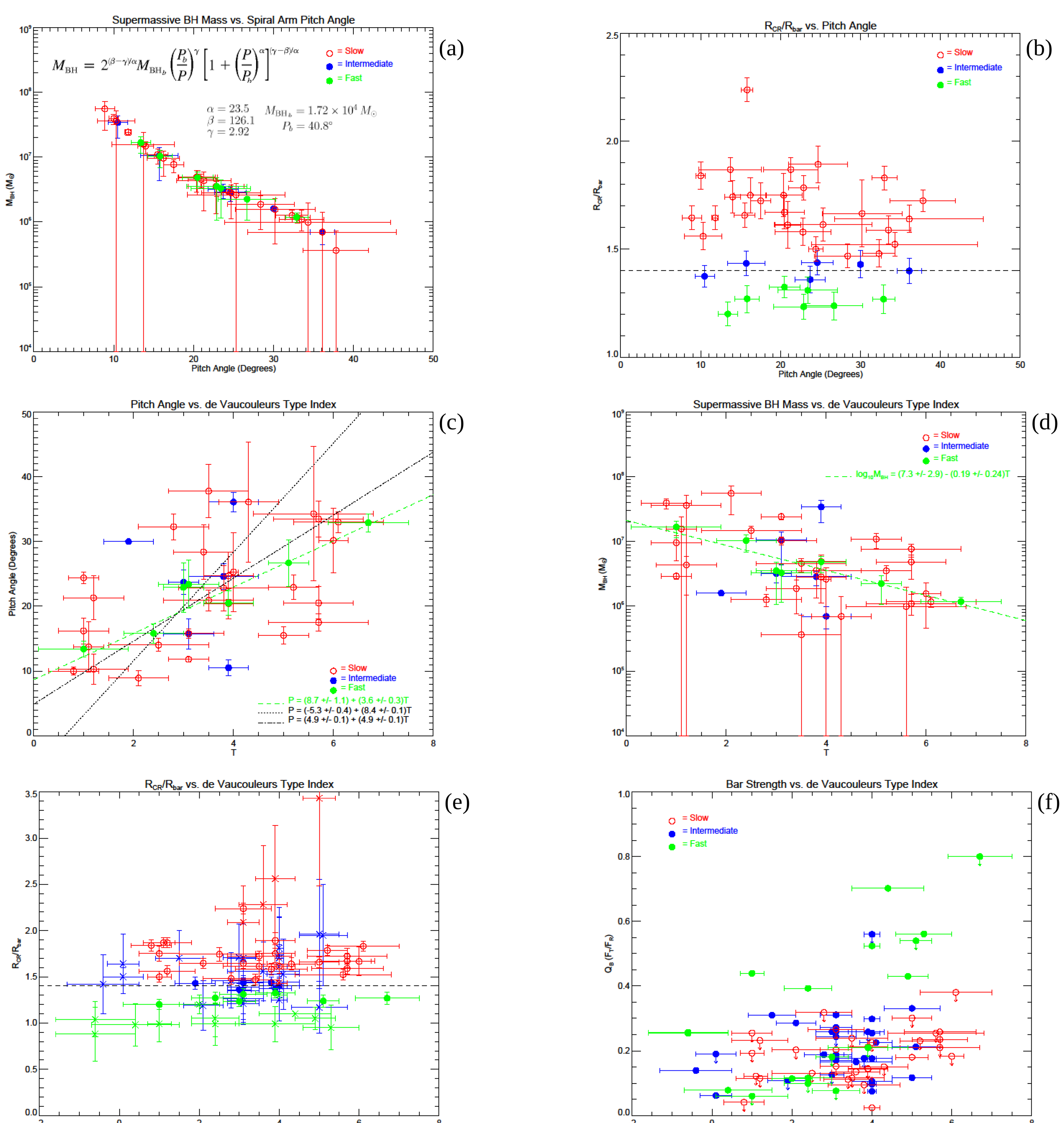

Figure 3: (a) Estimated SMBH mass vs. measured P. The fit given by equation 2 in Seigar et al. (2008) was applied to the data. (b) $\mathcal{R}$ vs. P. (c) P vs. T taken from HyperLeda. The dashed green line is a fit through the points corresponding to galaxies with fast bars, the dotted line is a fit through all the points, and the dot-dashed line is the fit predicted by Roberts et al. (1975). (d) SMBH mass vs. T. The dashed green line is the fit through the fast bar data points. (e) $\mathcal{R}$ vs. T. The points denoted by filled or open circles correspond to our data, while the crosses correspond to $\mathcal{R}$ data from Rautiainen et al. (2008). (f) Bar strength, Q_B, vs. T for a sample of four sets of galaxies including those listed in Table 1 and their corresponding Q_g, which may be treated as an upper limit estimate of Q_B; Table 1 and 2 of Rautiainen et al. (2008) and their corresponding Q_B (Buta et al. 2005); and Treuthardt et al. (2008, 2009) where Q_g was estimated by the authors.

CONCLUSIONS

We have determined the minimum M_{tot} values for a small sample of galaxies with clearly fast bars and therefore low central density dark matter halos. The minimum values are in the range of $3 < M_{tot} < 25 \times 10^{11}$ solar masses. It also appears that galaxies with low central dark halo densities appear to follow more predictable trends in P, or M_{BH}, versus de Vaucouleurs morphological type index (T) and bar strength versus T than barred galaxies in general. Future work will involve obtaining detailed rotation curves of the 7 galaxies with fast bars and determining if their M_{tot} do indeed exceed the predicted theoretical values.

REFERENCES

Bandara, K., Crampton, D., & Simard, L. 2009, ApJ, 704, 1135
Booth, C. M. & Schaye, J. 2010, MNRAS, 405, L1
Buta, R., Vasylyev, S., Salo, H., & Laurikainen, E. 2005, AJ, 130, 506
Debattista, V. P. & Sellwood, J. A. 2000, ApJ, 543, 704
Ferrarese, L. 2002, ApJ, 578, 90
Garcia-Gomez, C. & Athanassoula, E. 1993, A&AS, 100, 431
Ho, L. C., Li, Z.-Y., Barth, A. J., Seigar, M. S., & Peng, C. Y. 2011, ApJS, submitted
Kormendy, J. & Kennicutt, R. C., Jr. 2004, ARA&A, 42, 603
Rautiainen, P., Salo, H., & Laurikainen, E. 2008, MNRAS, 388, 1803
Roberts W. W., Roberts M. S., & Shu F. H., 1975, ApJ, 196, 381
Salo, H. 1991, A&A, 243, 118
Salo, H., Rautiainen, P., Buta, R., Purcell, G. B., Cobb, M. L., Crocker, D. A., & Laurikainen, E. 1999, AJ, 117, 792
Satyapal, S., Vega, D., Dudek, R. P., Abel, N. P., & Heckman, T. 2008, ApJ, 677, 926
Satyapal, S., Vega, D., Heckman, T., O'Halloran, B., & Dudek, R. 2007, ApJ, 663, L9
Schröder, M. F. S., Pastoriza, M. G., Kepler, S. O., & Puerari, I. 1994, A&AS, 108, 41
Seigar, M. S., Kennefick, D., Kennefick, J., & Lacy, C. H. S. 2008, ApJL, 678, 93
Treuthardt, P., Salo, H., & Buta, R. 2009, 137, 19
Treuthardt, P., Salo, H., Rautiainen, P., & Buta, R. 2008, AJ, 136, 300
van den Bosch, F. C., et al. 2007, MNRAS, 376, 841

This work was supported by a grant through the Arkansas NASA EPSCoR program and in part by the National Science Foundation under Grant CRI CNS-0855248, Grant EPS-0701890, Grant MRI CNS-619069, and OISE-0729792. We also acknowledge the use of the HyperLeda database and the NASA/IPAC Extragalactic Database (NED). The data presented in this paper were collected as part of the Carnegie-Irvine Galaxy Survey (CGS; http://cgs.obs.carnegiescience.edu) using facilities at Las Campanas Observatory, Carnegie Institution for Science. The optical data were reduced independently from those presented in Ho et al. (2011).